Technology for Analyzing Solute Carbon in Retained Austenite Using Soft X-ray Emission Spectroscopy

Dr. Aya HINO*1 • Keiko YAMADA*1

*1 Applied Physics Research Laboratory, Technical Development Group

Abstract

An attempt has been made to measure the microscopic distribution of carbon concentration and to analyze the results using a soft X-ray emission spectroscopy analyzer installed in a scanning electron microscope. The obstacle to accomplishing this was the organic substances adhering to the sample surfaces and acting as contaminants. However, a technique has been established for analyzing while removing contamination by gas-cluster ion beam irradiation, which has enabled carbon distribution measurement focusing on the microstructure in steel. It has also been suggested that this technique may be used for the analysis of the binding state of carbon contained in steel.

Introduction

As the world demands the reduction of CO_2 emissions, it is essential to reduce the CO_2 emitted by transport equipment. Weight reduction is one of the effective means for decreasing the amount of CO_2 emissions from transport equipment such as automobiles.

Reducing the weight of transport equipment, especially automobiles, requires steel sheets with high strength and workability. It is known that transformation-induced plasticity (hereinafter referred to as "TRIP") is effective in improving these properties. Murakami et al. have reported that the strength-elongation balance can be improved by controlling the concentration of solute carbon in retained austenite (retained γ) and dispersing it unevenly.[1] Their study estimates the unevenness of carbon concentration in retained γ from the peak shape of X-ray diffraction (XRD). However, the XRD method for identifying the amount of solid-dissolved carbon can analyze the average carbon content only in crystals with specific structures, but it cannot reveal the microscopic distribution of carbon concentration. Yamashita et al. have reported a method based on field emission electron probe micro-analysis (FE-EPMA) to analyze the carbon concentration distribution in a micro area of steel.[2] They consider that a higher spatial resolution is required to analyze the carbon concentration distribution in micro crystal grains in the order of several hundred nm. This paper reports the results of efforts to establish soft X-ray emission spectroscopy (hereinafter referred to as "SXES") for analyzing carbon at a spatial resolution of 200 nm or smaller in steel to study the carbon concentration distribution in micro crystal grains. Section 1 describes the apparatus configuration of SXES. Section 2 shows the results of examining the analysis conditions of SXES and introduces the contrast resolution and spatial resolution of SXES analysis. Section 3 describes the evaluation results using SXES on the solute carbon distribution in steel. Finally, Section 4 introduces future developments, focusing on the possibility of utilizing high energy resolution analysis, a feature of SXES.

1. Measurement apparatus

X-rays are emitted when inner shell electrons are excited by the electron beam irradiated on a sample surface, causing the transition of the valence band electrons. The SXES is a method for analyzing the energy spectrum in the soft X-ray region. The transition energy of electrons (released X-ray energy) has a value unique to the atomic species. Concerning electron transitions, the electrons that transition from the outermost shell to the inner shell have an energetic spread that reflects the state density of the electrons. From this aspect, it is said that SXES can analyze light elements with peaks on the low energy side and evaluate the bonding state of atoms.[3), 4)]

This study uses a scanning electron microscope (SEM)-equipped SXES detector (SEM: JEOL JSM-7100F, SXES: JEOL SS-94000) to perform SXES analysis with high spatial resolution. **Fig. 1** shows the apparatus configuration of the SXES used in this study.[5)] An electron beam irradiates the sample, and the soft X-ray in the generated X-rays is separated by a spectral grating and detected by two-dimensionally arranged CCD cameras. The spectral grating and the high-precision CCD cameras enable an analysis of soft X-rays with high energy resolution.

This study aims at establishing a method of quantitative analysis for solute carbon in steel. It is known; however, that an electron beam irradiated during SXES measurement causes contamination-containing carbon on the sample surface.[6)] The signal from the carbon contained in the contamination

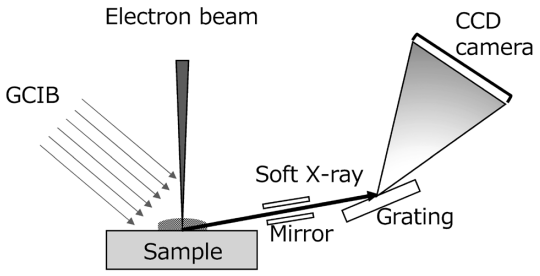

Fig. 1 Configuration of soft X-ray emission spectroscopic analyzer with scanning electron microscope

interferes with the measurement. Therefore, a gas cluster ion beam (GCIB) irradiation apparatus (GCIB10S manufactured by IONOPTIKA) has been attached to the SXES apparatus for decontamination,[7)-9)]

The conditions for SXES measurement are acceleration voltage 5 kV and measurement time 5 min/point, unless otherwise specified.

2. Examination of analysis conditions and results of analyzing steel

2.1 Quantitative evaluation of carbon and creation of standard curve

This section evaluates the correlation between carbon content and SXES spectral intensity. Also described is the creation of the standard curve. The samples are Fe-C thin films in which the carbon content in the Fe was controlled. The sputtering method, which facilitates the formation of metastable states, was selected for sample preparation. The samples were formed by simultaneous sputtering with Fe and C targets. The carbon contents calculated from the thickness (volume) and density of the films deposited from the targets were 0.00, 1.00, 1.10, 1.19, 1.40, 1.58, and 2.47 mass%. The intensity of second-order C Kα was obtained from the SXES spectrum of the Fe-C thin films. To this end, the difference in the measurement results between the Fe thin film and the SXES of each Fe-C thin film were taken to derive the integrated intensity of the second-order C Kα. **Fig. 2** shows the relationship between the carbon contents in the samples and the integrated intensity of the second-order C Kα of SXES. A linear relationship was found in the integrated intensity of carbon content and second-order C Kα, allowing the creation of a standard curve.

The standard deviation σ in the simple regression model of the standard curve was determined by Equation (1), and the quantitative accuracy σ_c for the carbon was obtained by Equation (2), assuming the variation in the carbon content of the sample:[10)]

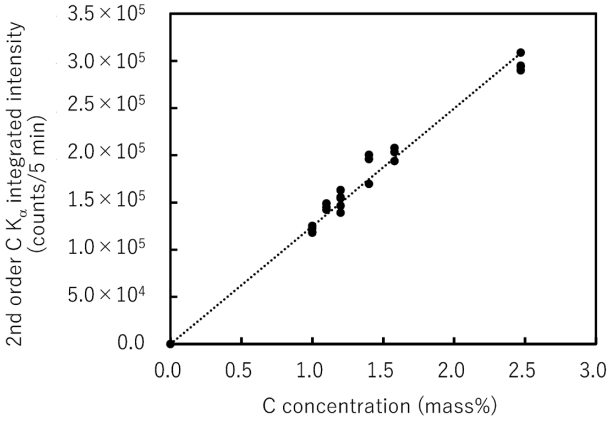

Fig. 2 Standard curve between 2nd order C Kα integrated intensity and C concentration for Fe-C film

$$\sigma = \sqrt{\frac{\sum_{i=1}^{n}[\{y_i - (\hat{\alpha} + \hat{\beta}x_i)\}^2]}{n-2}} \quad \cdots\cdots (1)$$

$$\sigma_c = \frac{\sigma}{\hat{\beta}} = 0.091 wt\% \quad \cdots\cdots (2)$$

wherein y_i is the count number of second-order C Kα of the i-th data, $\hat{\alpha}$ is the y-intercept of the regression line, $\hat{\beta}$ is the slope of the regression line (count/mass%), x_i is the carbon concentration (mass%) of the i-th data, and n is the number of measurement points.

The quantitative accuracy has turned out to be 0.091 mass%, considering the sample's carbon content variation, showing that the SXES can discriminate the difference in the carbon content of 0.1 mass%.

2.2 Removal of carbon-containing contaminant and line mapping analysis

This section introduces efforts to establish a measuring method that is not affected by carbon-containing contaminants, which adhere during SXES measurement. TRIP steel (steel A) consisting of equiaxial fine grains was used as the sample to examine an analysis method with decontaminating capability. The GCIB, used for cleaning off organic matter, was examined to remove the contaminants that adhere during the measurement.

First, to investigate the decontamination effect of GCIB, line measurement by SXES and SEM observation were performed with and without GCIB irradiation. The measurement was focused on an α grain (carbon concentration 0.02 mass% or less) in steel A, and the influence of the variation in the sample's carbon concentration was excluded. The interval of the line measurement was 150 nm, and the total measurement length was 2 μm.

The SEM images of the sample surfaces after SXES line measurement are shown in **Fig. 3** (a) without GCIB and Fig. 3 (b) with GCIB. The white dotted line in Fig. 3 indicates the location of the line measurement. Fig. 3 (a) shows adhesion around the line measurement location, presumed to be a contaminant. On the other hand, in Fig. 3 (b), no adhesion is observed on the sample's surface.

Fig. 4 shows the second-order C Kα integrated intensity measured by the SXES line measurement. Without GCIB, the integrated intensity of the second-order C Kα increased sharply after the second measurement and did not decrease until the end of the measurement. On the other hand, with GCIB, the second-order C Kα integrated intensity exhibits almost no change. There is almost no distribution of carbon in the α grain used for the measurement, and the increase in the integrated intensity of the C Kα second-order line seen without GCIB is unlikely to be derived from the sample. Thus, the measurement results obtained with GCIB are considered to match the sample properties. The results shown in Fig. 3 and Fig. 4 have led to an SXES measurement method with GCIB irradiation to remove contaminant that adheres to the sample surface by electron beam irradiation.

2.3 Spatial resolution of SXES analysis in steel

A spatial resolution of several hundred nm or smaller is required to evaluate the carbon concentration distribution in the retained γ of steel. This section describes the evaluation of SXES's spatial resolution in steel. This study aims at a spatial resolution of 200 nm or smaller in steel. The spatial resolution was evaluated by the line measurement of steel A used in the previous section. The SXES line measurement location of steel A is shown in **Fig. 5** (a), and the analysis results are shown in Fig. 5 (b). As shown in Fig. 5 (a), the line measurement location straddles the point where α grain and retained γ grain touch. As shown in Fig. 5 (b), the integrated intensity of the second-order C Kα changes in accordance with the locations between the α grain and retained γ grain in steel A. The concentration variation at the boundary between

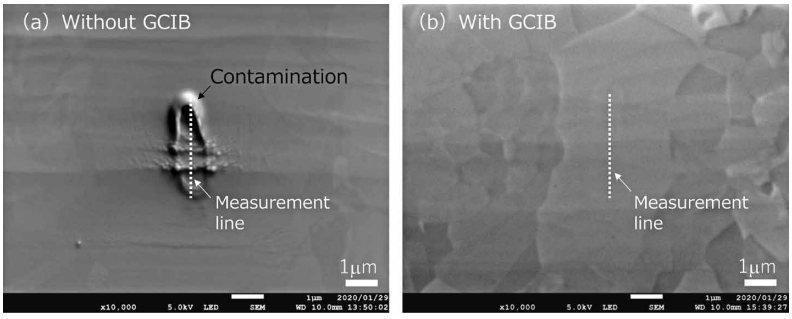

Fig. 3 SEM images of samples (a) without GCIB and (b) with GCIB after SXES line measurements

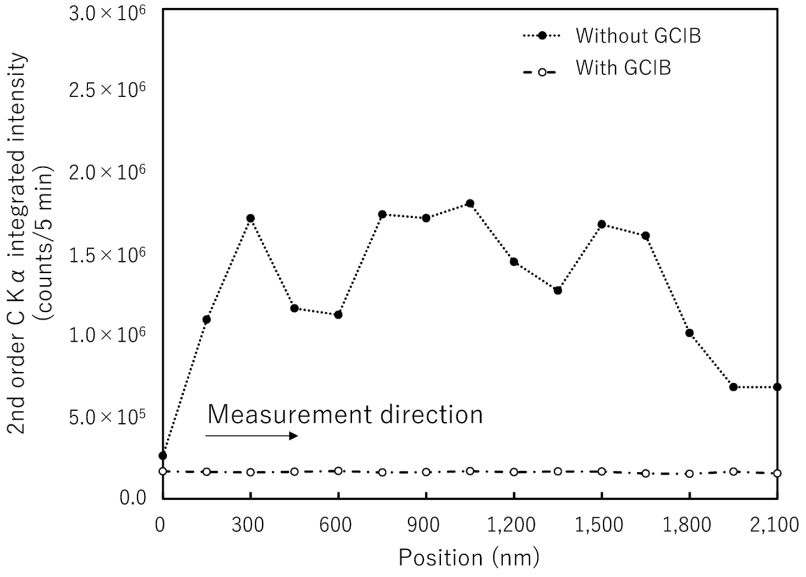

Fig. 4 Variation of 2nd order C Kα integrated intensity of SXES line measurements with and without GCIB

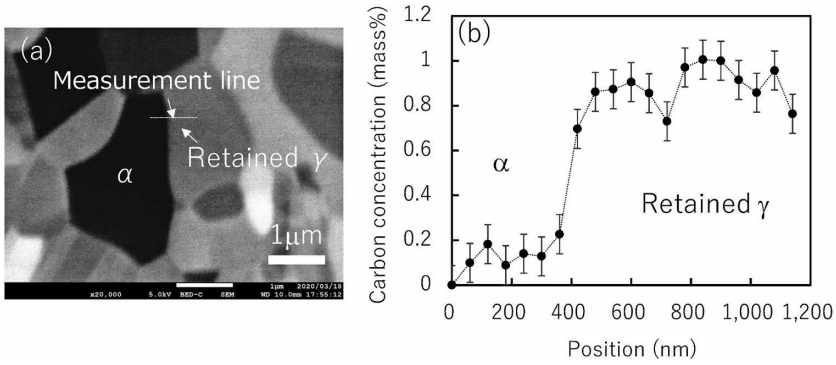

Fig. 5 (a) SEM image and (b) SXES line measurement results of steel A sample including α and retained γ phase

α grain and retained γ grain is described by measurements at 4 points or less. Hence, the actual spatial resolution of SXES during the measurement is estimated to be 180 nm or smaller, which is the distance covered by the four measurement points. This verifies that the spatial resolution in the steel of the SXES analysis measured this time is 180 nm or smaller.

3. Analysis and evaluation of carbon in steel microstructure

The above study has enabled a contrast resolution in steel of 0.1 mass% or smaller and spatial resolution of 180 nm or smaller in SXES analysis. This section describes an attempt to evaluate the microscopic distribution of solute carbon in retained γ in steel. A sample of 1.5 GPa class TRIP steel with a carbon content of 0.4 mass% (steel B) was evaluated for the concentration distribution of solute carbon in the retained γ in the steel microstructure. **Fig. 6** (a) shows steel B's electron backscatter diffraction (EBSD) phase map. In the figure, the red corresponds to α grains, and the green corresponds to retained γ grains. The SXES analysis was performed at the points identified as being in retained γ grains. Fig. 6 (b) shows the frequency distribution of the solute carbon concentrations in the retained γ grains of the steel B. As shown in this figure, the carbon content distribution of retained γ grain in steel B is divided into grains with 1.2 mass% or lower and grains with 1.4 mass% or higher. No clear correlation between carbon distribution and grain size has been found in this measurement.

In the frequency distribution shown in Fig. 6 (b), grains with a carbon concentration close to 0 mass% have been detected, although they are retained γ grains. Usually, no grain with low carbon content remains as a retained γ grain; however, this measurement has detected retained γ grains with low carbon content. The following discusses

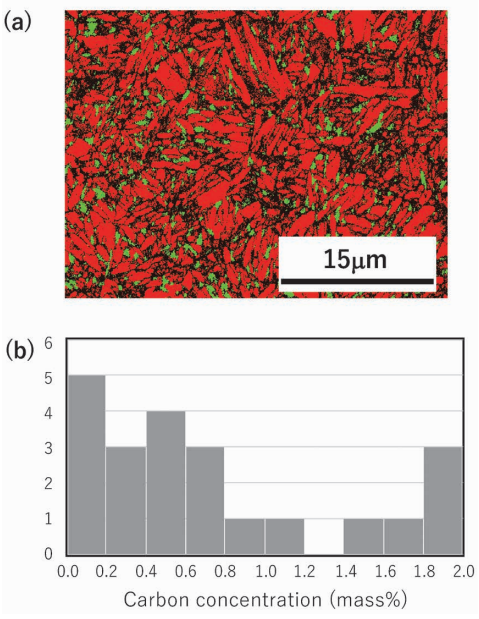

Fig. 6 (a) Phase map image of steel B sample by using EBSD (red: body center cubic, green: face center cubic) and (b) histogram of carbon concentration in retained γ phase measured by SXES

the reason. In the case of SXES measurement, the electron penetration depth into the sample is estimated to be approximately 160 nm from the equation of Kanaya and Okayama.[11), 12)] If a retained γ grain is thin in the depth direction from the sample surface and α grain is present below it, the carbon content is presumed to be intermediate following the volume ratio of the α grain and retained γ grain. Since the distribution of grains in the depth direction of the sample cannot be evaluated, it is considered necessary to improve future measurement and sample preparation methods.

Per the analysis above, SXES-equipped SEM combined with GCIB enables carbon concentration analysis focusing on each retained γ grain in steel, which has yielded a measurement result indicating that the concentration of solute carbon is different for each grain.

4. Prospects: Toward the evaluation of bonding state

Carbon is a typical element that strongly affects steel's properties. The state of carbon in the steel, such as solid solution or carbide, greatly influences delayed fracture and workability. Hence, an SXES analysis has been performed on steel consisting of a lamellar perlite structure (steel C) to evaluate the bonding state of carbon in the steel. **Fig. 7** (a) shows an SEM image of steel C, and Fig. 7 (b) shows its SXES mapping image. As shown in Fig. 7 (a), steel C has a lamellar structure. The SEM image presents a lamellar structure consisting of a bright contrast α layer and a dark contrast Fe_3C layer. This image has been mapped with SXES at 1 min/point, which yielded the image shown in Fig. 7 (b). In Fig. 7 (b), the high-carbo-content region is shown in red, producing a color contour diagram of the lamellar structure corresponding to the SEM image.

The spot measurement results on the solute carbon in steel A's retained γ grain, steel A's α grain, and steel C's Fe_3C in lamellar perlite have been standardized by min/point to produce the spectra shown in **Fig. 8**. The results show that the spectral intensity of approximately 138 eV is the strongest for the solute carbon in the retained γ grain, and approximately 139 eV is the strongest for the carbon in Fe_3C. The spectral shapes differ between the solute carbon in the retained γ and the carbon in Fe_3C. The above indicates that the SXES can detect a spectrum that reflects the difference in the state of carbon in the steel, a possibility of analysis that reflects the bonding state of carbon in steel by SXES.

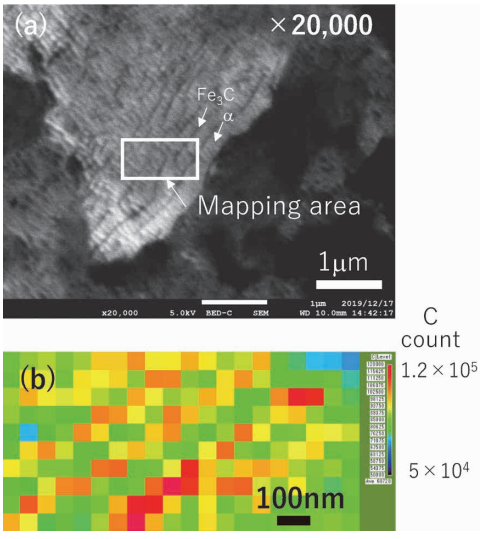

Fig. 7 (a) SEM image and (b) carbon concentration mapping image of lamellar perlite by using SXES

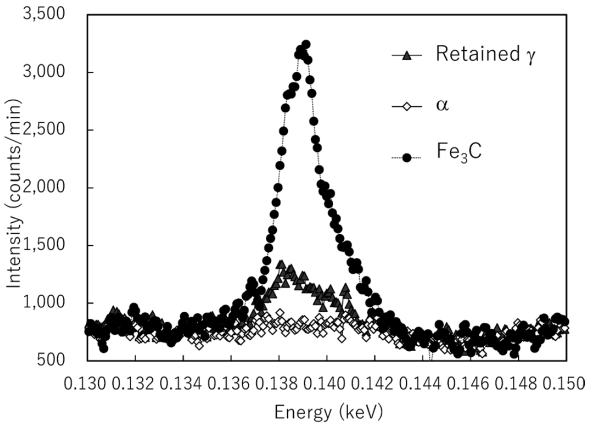

Fig. 8 2nd order C Kα spectra of solute C in retained γ, α, and Fe_3C obtained by using SXES

Conclusions

This study has established a method using SEM with SXES to analyze the steel's microscopic solute carbon quantitatively. The GCIB irradiation has successfully removed contamination containing carbon that adheres to the sample surface during the measurement, a problem in analyzing solute carbon in the steel, offering a clear idea for measuring the carbon concentration distribution in each micro-crystal grain of the steel. Kobe Steel will utilize these analysis techniques to develop materials such as steel.

This paper is based on results obtained from a project, JPNP14014, commissioned by the New Energy and Industrial Technology Development Organization (NEDO).

References

1) T. Murakami. R&D Kobe Steel Engineering Reports. 2019, Vol.69, No.1, pp.29-32.
2) T. Yamashita et al. Tetsu-to-Hagane. 2017, Vol.103, No.11, pp.622-628.
3) M. Terauchi et al. J. Surf. Sci. Soc. Jpn. 2015, Vol.36, No.4, pp.184-188.
4) K. Tanaka. Bulletin of the Japan Institute of Metals. 1976, Vol.15, No.12, pp.753-761.
5) M. Terauchi et al. Handbook of Soft X-ray Emission Spectra Version 5.0. JEOL Ltd., 2019, p.11.
6) M. Amman et al. Journal of Vacuum Science & Technology B.1996, Vol.14, Issue1, pp.54-62.
7) I. Yamada et al. OYO BUTURI. 1997, Vol.66, No.6, pp.559-568.
8) A. Miisho. Tech_library KOBELCO research institute. 2015, No.43 APR, pp.1-3.
9) T. Miyayama. Journal of the Vacuum Society of Japan. 2016, Vol.59, No.5, pp.134-137.
10) T. Kubokawa et al. Statistics. University of Tokyo Press, 2016, p.352.
11) K. Kanaya et al. Journal of Physics D. 1971, Vol.5, No.1, pp.43-58.
12) H. Soejima. J. Surf. Sci. Soc. Jpn. 1984, Vol.5, No.3, pp.351-363.